



**HAL**  
open science

## **Self-Biasing Effects Induced by RF Step-Stress in Ka-Band LNAs based on InAlN/GaN HEMT Technology**

Jean-Guy Tartarin, Séraphin Dieudonné Nsele, S Piotrowicz, S Delage

### ► **To cite this version:**

Jean-Guy Tartarin, Séraphin Dieudonné Nsele, S Piotrowicz, S Delage. Self-Biasing Effects Induced by RF Step-Stress in Ka-Band LNAs based on InAlN/GaN HEMT Technology. 11th European Microwave Integrated Circuits Conference (EuMIC 2016), Oct 2016, Londres, United Kingdom. <10.1109/EuMIC.2016.7777596>. <hal-02088210>

**HAL Id: hal-02088210**

**<https://laas.hal.science/hal-02088210v1>**

Submitted on 2 Apr 2019

**HAL** is a multi-disciplinary open access archive for the deposit and dissemination of scientific research documents, whether they are published or not. The documents may come from teaching and research institutions in France or abroad, or from public or private research centers.

L'archive ouverte pluridisciplinaire **HAL**, est destinée au dépôt et à la diffusion de documents scientifiques de niveau recherche, publiés ou non, émanant des établissements d'enseignement et de recherche français ou étrangers, des laboratoires publics ou privés.



HAL Authorization

# Self-Biasing Effects Induced by RF Step-Stress in Ka-Band LNAs based on InAlN/GaN HEMT Technology

J.G. Tartarin, S.D. Nsele

LAAS-CNRS and University of Toulouse (UPS)  
F31-031, Toulouse, France  
tartarin@laas.fr

S. Piotrowicz, S. Delage

Thales Research Technology, III-V Lab  
Palaiseau, France

**Abstract**— Nitride technologies are proposing a large variety of active devices to address high-power modules, but also robust low-noise receivers at high frequencies. High Electron Mobility Transistors (HEMT) are essentially developed on AlGaIn/GaN heterostructure, but InAlN/GaN alternative seems very promising due to lattice matched layers (using 17% of In content) at the interface between layers where the channel (2DEG) occurs, and to a better mobility in the 2DEG. This paper presents a study on Ka-band Low Noise Amplifiers featuring a Noise Figure of 3.3dB between 29-30.5 GHz for the single stage version under study. RF step-stresses and CW stresses have been applied on four different LNAs, evidencing fluctuation of charges in the active device. Self-biasing of the HEMT is emphasized and assessed through the evaluation of the 2<sup>nd</sup> order harmonic at 59 GHz. Initial noise and dynamic performances can be fully recovered after a long period with no RF signal, or by applying a positive voltage on the gate to remove charges under the gated zone of the transistor. These results on the stability of the noise figure of LNAs prove that jamming signals can be harmless on GaN based receivers, even if some more improvements have to be achieved on these not yet mature technologies.

**Keywords**—component; GaN HEMT, InAlN/GaN, LNA, Noise Figure, Ka-band, step-stress, CW stress.

## I. INTRODUCTION

High power amplifiers used in wireless telecommunication or radar applications have motivated the development of wide bandgap emerging technologies. Electrical performances and thermal budgets position these technologies as a major competitor for power segment modules, through the development of solid state power amplifiers (SSPA). On the other hand, the ability of these technologies to endure high input power is also a key-point to address in robust receivers: the development of robust low noise amplifiers (LNA) represents a challenging aspect for developing high frequency, high power and low noise GaN technologies. If AlGaIn/GaN high electron mobility transistors (HEMT) are still suffering from a lack of reliability (some failures are attributed to lattice defects resulting from the mismatch and from the piezoelectric effects), InAlN/GaN HEMT is expected to improve the mechanical stability of the heterostructure, and thus the reliability of the transistor. Moreover, a higher output current density can lead to a higher power density if the breakdown voltage is preserved. The targeted application concerns Ka-

band transceivers. Different versions of LNAs have been developed on the optimized nitride technology. In this paper, a one-stage LNA has been investigated under small-signal and large signal conditions versus RF CW and step-stresses in Ka-band. In the next section, the high-frequency dynamic and noise performances of the transistor are presented. The third section presents the design and the performances of the 1-stage LNA. The last paragraph concerns the electrical behavior of the LNA versus RF input signal at 29.5 GHz for CW and step-stresses.

## II. INALN/GAN MOS-HEMT TECHNOLOGY

The transistors used to design the LNAs are InAlN/GaN HEMTs and MOS-HEMTs grown on 3 inches SiC substrate by using the MOCVD technique. The technological process has been optimized considering the transition frequency  $f_t$  and maximum oscillation frequency  $f_{max}$ , the output power at the 1 dB compression point and the HF noise figure (NF) for Ka-band applications.  $f_t = 40$  GHz and  $f_{max} = 110$  GHz have been achieved for the MOS-HEMT process used to design the Ka-band amplifiers of this study. Power densities of 3.5 W/mm and power added efficiencies of 40 % have been measured at 30 GHz on 0.15  $\mu\text{m}$  gate length devices (6 $\times$ 50  $\mu\text{m}$  gate width). The optimum low noise sizing and biasing conditions have been obtained for a 0.15  $\mu\text{m}$  gate length device featuring 2 $\times$ 75  $\mu\text{m}$  gate width, biased at  $V_{DS} = 6$  V and  $I_{DS} = 20$  mA; a minimum noise figure of  $F_{min} = 2$  dB with an associated gain of 7.5 dB are measured at 30 GHz [1].

## III. ROBUST KA-BAND LNA DESIGNS

Different LNA versions have been designed using hybrid (MIC) and monolithic (MMIC) technologies. This paper focuses on the study developed for the one-stage hybrid LNA which allows the analysis of the single transistor contribution to the electrical performances of the LNA when subjected to RF stresses. MOS-HEMTs are flip-chipped on alumina substrate, with via holes to interconnect the ground to the metal board. The MIC circuit layout (without flip-chipped transistor) is presented in Fig. 1, and the final LNA photograph is proposed in Fig. 2.

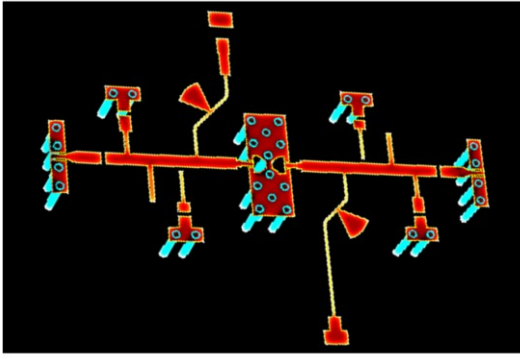


Fig. 1. Layout of the LNA (MIC with via holes and flip-chip footprint of the transistor, input and output coplanar pads for GSG probe contact).

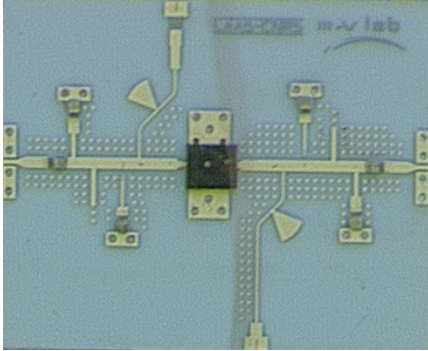


Fig. 2. Photograph of the 1-stage Ka-band LNA (flip-chipped mounted InAlN/GaN MOS-HEMT, biased at  $V_{DS} = 6$  V,  $I_{DS} = 20$  mA). Total size of the circuit is  $9 \times 7.5$  mm<sup>2</sup>.

Flip-chip report of the active device is convenient to reduce the transistor-to-circuit connection lengths and associated losses. Moreover, the connections by bumps can act as thermal bridges to dissipate the heat from the transistor's active zone. The small wavelength at 30 GHz makes possible the use of distributed matching and design techniques. For this study, four different amplifiers have been assembled and characterized. Noise figures have been measured between 3.3 dB and 3.9 dB at 29.5 GHz over the four LNAs, which is 0.3 dB above the simulated value. The gain measurements at 29.5 GHz range between 6.1 dB and 6.7 dB for three LNAs (one amplifier features a marginal 3.7dB gain). The noise figure for the 1-stage LNA is reported in Fig. 3, with other works based on GaN technologies and compiled from literature [2]-[12]. Few LNAs have been designed in the Ka-band, and this work presents state of the art figure of merit with the NF measured at 3.3 dB (MIC 1-stage LNA), despite using a relatively immature technology.

Three stages LNAs have also been designed using the same device sizing and biasing, in MMIC technology (GH25 design kit from UMS). For these MMIC LNA designs (3mm<sup>2</sup>), much more flexibility is allowed in comparison with hybrid circuits as the source contact allows fine adjustment of serial feedback since it is also possible to mix lumped elements and transmission lines. For this reason, very competitive noise figures are achieved: Noise Figures of 3 dB and 2.6 dB were simulated for the LNAs respectively using lumped and

distributed lines at 30 GHz (for small signal gain above 20dB and input/output reflection coefficient lower than -10dB over 26-34 GHz) [13].

For this study, only single-stage hybrid LNAs have been tested versus CW and RF stresses at 30 GHz.

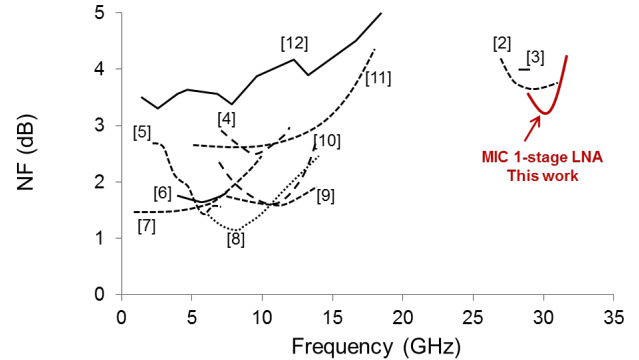


Fig. 3. State-of-the art in GaN LNA technologies. References are largely inspired from [2]. This work reports InAlN/GaN based LNA

#### IV. RF STRESSES IN KA-BAND

The robustness assessment of a LNA based on III-N technologies can be developed by applying thermal stresses, CW stresses at several compression points, or step-stresses to evaluate the behavior of the amplifier under a harsh or critical operating environment. In this paper, RF stresses have been applied at 29.5 GHz, using an Anritsu MG3694B 40 GHz synthesizer and a 67 GHz Rohde & Schwarz spectrum analyzer was used for fundamental and 2<sup>nd</sup> harmonic power detection.

##### A. Stress under 29.5GHz CW signal at 4dB compression point

After a power characterization ( $P_{out} - P_{in}$  at 29.5 GHz featuring  $P_{1dB} = 10$  dBm for the LNA reported in this study), the LNA has been stressed by a CW signal at 4 dB compression over 32 hours (Fig. 4 represents the first 24 hours). A rapid decrease of the DC drain current (more than 10 %) in the first 5 hours can be correlated to the reduction of 0.6 dB in the compressed signal of the fundamental tone. Surprisingly, the DC drain current still decreases according to a monotonous trend (quasi Neperian logarithmic law) whereas the output compressed power at 29.5 GHz fluctuates by more than 1.5 dB and then remains constant at 2 dB under the initial gain value (no manual data collection between 10h and 15h in Fig. 4). From different studies in a lower frequency range, it has been proved that the InAlN/GaN MOS-HEMT is very sensitive to charges located in the gate-drain and gate-source regions (evidenced by LF noise and HF frequency dispersion on both the transconductance gain  $g_m$  and output dynamic conductance  $g_{DS}$ ) [14][15]. The application of a large signal during long stress periods can activate secondary generators (self-biasing) that makes the output power fluctuate. The power-slump evidenced on this amplifier, correlated to a reduction of the carrier density in the 2DEG, has also been

evidenced on GaN technologies [16] and GaAs devices under large signal operation [17].

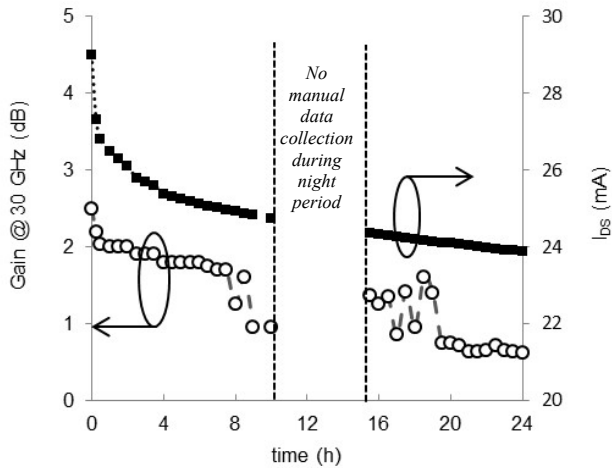


Fig. 4. Gain variation at 29.5 GHz and DC drain current versus time for a single stage LNA under non-linear CW RF signal (@ 4 dB compression point).

When the RF generator is set from On to Off state, the DC drain current instantaneously shifts from 20 mA (initial biasing value) to 15 mA (Fig. 5). Then, when setting the RF signal On again, the DC current increases up to 30mA. From these instantaneous shifts at each cycle,  $I_{DS}$  evolves with time. Different measurements have been performed (periods of 20 minutes for each cycle, 2 cycles for each On-Off RF signal are represented in Fig.5). This test proves that self-biasing occurs around the 20 mA initial DC biasing, with long recovery times involved: the evolution of DC biasing and RF signal also present a correlated general trend in Fig. 5, but RF gain fluctuations due to carriers trapped from the 2DEG also feature non-monotonous trends. Finally, more than an hour is needed to recover the initial DC drain current after RF signal shutdown. It can also be noticed that a positive gate voltage  $V_{GS} = 2$  V removes instantaneously ( $< 1$  sec) the charges under the gate and in the gate-drain region, and the initial DC quiescent point is recovered.

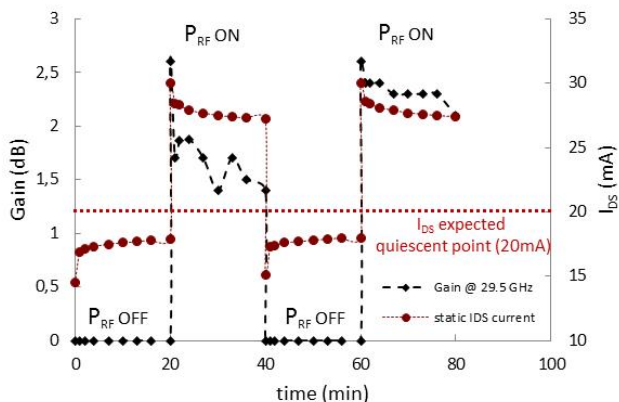


Fig. 5. Gain at 29.5 GHz and DC drain current variations versus time for a single stage LNA under non-linear CW RF signal (@ 4 dB compression point). RF signal is turned ON and OFF alternately every 20 minutes.

### B. Step-Stress under a 29.5 GHz CW signal

Step stresses have been applied on two LNAs. Both were featuring a systematic change in DC drain current. For an RF input power between 10 and 14 dBm, i.e. when the transistor runs under compression, the DC drops down to 15 mA and keeps this value (same conditions as for CW stress under 4 dB compression). Several measurements have been performed to assess the validity of the measurements (7 iterations for each LNA). The duration of each RF step is 2 minutes, with 2 dB incremented RF input power. From measurements of the second harmonic power at 59 GHz (Fig. 6), the DC self-biasing parameter change due to RF signal application can be extracted.

The second harmonic variation law is the same as the nonlinear induced DC variation under large signal, considering the well-known linearization of  $\cos^2(x)$  given in (1), and then used to compute the quadratic function for the DC self-biasing contribution through the extraction of  $b$  coefficient from (2) (limiting the polynomial expression to order 3).

$$\cos^2(\alpha t) = [1 + \cos(2\alpha t)]/2 \quad (1)$$

$$P_{OUT} = a \cdot P_{IN} + b \cdot P_{IN}^2 + c \cdot P_{IN}^3 \quad (2)$$

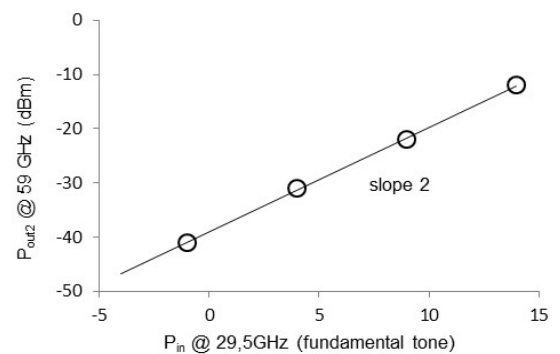


Fig. 6. Evolution of the 2<sup>nd</sup> harmonic signal (@ 59 GHz) under different input power (fundamental tone @ 29.5 GHz, cf. table 1)

Since the output power for the second harmonic can be expressed by the same coefficient  $b$  as for the DC self-biasing contribution, different elements given in table 1 can be computed. The RF voltage swing  $V_{GS-RF}$  on the gate is calculated from the input power  $P_{IN}$  delivered at the matched input of the LNA,  $b$  coefficient is derived from the output second harmonic  $P_{OUT2\_2nd\ harmonic}$ , and DC self-biasing gate voltages and drain current are estimated from the I-V load-line. The analysis of Fig. 6 leads to the extraction of  $b = 0.25$  for powers up to 10 dBm ( $b = 54$  for  $P_{IN} = 14$  dBm, which cannot be used). Table 1 reports the different electrical parameters measured ( $P_{IN}$ ,  $P_{OUT2\_2nd\ harmonic}$ , DC measured  $\Delta I_{DS}$ ) and computed ( $V_{GS-RF}$  @29.5GHz,  $b$  coefficient, DC self-biasing  $\Delta V_{GS}$  and  $\Delta I_{DS}$ ): when using  $b = 0.25$  coefficient, self-biasing  $\Delta V_{GS}$  and  $\Delta I_{DS}$  are correctly computed for our RF

stresses (CW and step-stress), and is also coherent with the  $I_{DS}-V_{DS}$  static output characteristics of the devices. Good agreement is obtained with the measured  $\Delta I_{DS}$  variation of the drain current of the LNA.

Finally, after several RF tests (more than 10 step-stresses and CW stresses), it has been evidenced that no degradation is noticeable on the small-signal gain, on  $P_{1dB}$  or on the noise figure after the transistors have recovered their initial quiescent biasing point. No permanent degradation has been evidenced during these stresses. It can be noticed that DC conditions are low voltage and low current to match low noise requirements; thus no DC stress occurs in the active devices, contrary to tests performed at high DC power for large-signal applications.

TABLE I  
SELF-BIASING EFFECT DUE TO LARGE-SIGNAL RF POWER

$P_{IN}$ (29.5 GHz)	-1 dBm	+4 dBm	+9 dBm	+14 dBm
$V_{GS-RF}$ @29.5 GHz	0.282V	0.5V	0.9V	1.6V
$P_{OUT2\_2nd}$ harmonic	-41 dBm	-31 dBm	-22 dBm	-17.5 dBm
$b$ coefficient	0.25	0.256	0.21	(using 0.25)
DC self-biasing $\Delta V_{GS}$	0.003 V	0.009 V	0.025 V	0.33 V
DC computed $\Delta I_{DS}$	0mA (0%)	1mA (7%)	5mA (33%)	13mA (90%)
DC measured $\Delta I_{DS}$	0mA	0.7mA	6mA	15mA

## V. CONCLUSION

Ka-band LNAs using InAlN/GaN (MOS-)HEMT devices have been characterized at 29.5 GHz, featuring a state of the art noise figure of  $NF = 3.3$  dB. Radio frequency CW stresses have been performed on different LNAs, evidencing self-biasing effects due to the activation of charges in the gated zone of the transistor under large-signal conditions; very long recovery time constants are evidenced. A simple intuitive model has been developed to account for the self-biasing effect occurring in active devices, which matches the different RF CW and step stresses experiments performed on amplifiers. Finally, after those RF stresses, once the DC initial conditions are recovered, no degradation is noticed in the gain, in the compression point or in the noise figure of the low-noise amplifiers under test.

## ACKNOWLEDGMENT

This work was partially supported by the Genghis Khan Project in the Framework of the French Research National Agency. The authors also acknowledge all the other partners of the project (Thales Communication, EGIDE, United Monolithic Semiconductors and Institut Lavoisier) for fruitful exchanges and discussion, and Professor L. Escotte from LAAS-CNRS for his active contribution to the characterization of HF noise parameters and transistor's modelling.

## REFERENCES

[1] S.D. Nsele, J.G. Tartarin, L. Escotte, S. Piotrowicz, S. Delage, "InAlN/GaN HEMT Technology for Robust HF Receivers: an Overview of the HF and LF Noise Performances" *International Conference on Noise and Fluctuation, ICNF 2015, X'ian, China, 4 p.*

[2] M. Rudolph, N. Chaturvedi, K. Hirche, J. Würfl, W. Heinrich, G. Tränkle, "Highly rugged 30 GHz GaN low-noise amplifiers," *IEEE Microwave and Wireless Components Lett.*, vol. 19, no. 4, pp. 251-253, 2009.

[3] E.M. Suijker, J.A. Hoogland, M. Van Heijningen, M. Seelman-Eggebert, R. Quay, P. Bruckner, F.E. Van Vliet, "Robust AlGaIn/GaN Low Noise Amplifier MMICs for C-, Ku- and Ka-band space applications," *IEEE Compound Semiconductor Integrated Circuit Symposium*, 2009. CISC 2009. 4p.

[4] M. Micovic, A. Kurdoghlian, H.P. Moyer, P. Hashimoto, A. Smits, I. Milosavljevic, P.J. Willadsen, W.S. Wong, J. Duvall, M. Hu, M. Wetzel, D.H. Chow, "GaN MMIC technology for microwave and millimeter-wave applications" in *Proc. IEEE Compound Semiconductor Int. Circuits Symp. CSIC*, 2005, pp. 173-176.

[5] M. Rudolph, R. Behtash, K. Hirche, J. Würfl, W. Heinrich, G. Tränkle, "A high survivable 3-7 GHz GaN Low-Noise Amplifiers," *IEEE MTT-S Int. Dig.*, 2006, pp. 1899-1902.

[6] H. Xu, C. Sanabria, A. Chini, S. Keller, U.K. Mishra, R.A. York, "A C-band high-dynamic range GaN HEMT low-noise amplifier," *IEEE Microwave Wireless Component Letters*, Vol. 14, no.6, pp.262-264, June 2004.

[7] M.V. Aust, A.K. Sharma, Y.C. Chen, M. Wojtowicz, "Wide-band dual-gate GaN HEMT low noise amplifier front-end receiver electronics," in *Proc. IEEE Compound Semiconductor Int. Circuits Symp. CSIC*, 2006, pp. 89-92.

[8] J.C. De Jaeger, S.L. Delage, G. Dambrine, M.A. Di Forte Poisson, V. Hoel, S. Lepilliet, B. Grimbert, E. Morvan, Y. Mancuso, G. Gauthier, A. Lefrançois, Y. Cordier, "Noise assessment of AlGaIn/GaN HEMTs on Si or SiC substrates: application to X-band low noise amplifiers," in *Proc. European Gallium Arsenide Other Semiconductors Appl. Symp. 2005*, pp. 229-232.

[9] D. Krausse, R. Quay, R. Kiefer, A. Tessman, H. Massler, A. Leuther, T. Merkle, S. Müller, C. Schworer, M. Mikulla, M. Schlechtweg, G. Weiman, "Robust GaN HEMT low-noise amplifier MMICs for X-band applications," in *Proc. European Gallium Arsenide Other Semiconductors Appl. Symp. 2004*, pp. 71-74.

[10] R.S. Schwindt, V. Kumar, O. Aktas, J.W. Lee, I. Adesida, "Temperature-dependence of a GaN-based HEMT monolithic X-band low-noise amplifier," in *Proc. IEEE Compound Semiconductor Int. Circuits Symp. CSIC*, 2004, pp. 201-204.

[11] G.A. Ellis, J.S. Moon, D. Wong, M. Micovic, A. Kurdoghlian, P. Hashimoto, M. Hu, "Wideband AlGaIn/GaN HEMT MMIC low noise amplifier," in *IEEE MTT-S Int. Digest*, 2004, pp.153-156.

[12] S. Colangeli, A. Bentini, W. Ciccognani, E. Limiti, A. Nanni, "GaN-based robust Low-Noise Amplifiers" *IEEE Trans. On Electron Devices*, Vol.60, no.10, October 2013, pp. 3238-3247. Ketterson, E. Beam, M. Pilla, X. Gao, "InAlN barrier scaled devices for very high  $f_T$  and low-voltage RF applications," *IEEE Trans. Electron Devices*, vol. 60, no. 10, pp. 3099-3104, 2013.

[13] S. Nsele, C. Robin, J.G. Tartarin, L. Escotte, O. Jardel, S. Piotrowicz, S. Delage, "Ka-band Low Noise Amplifiers based on InAlN/GaN technologies", *International Conference on Noise and Fluctuation, ICNF 2015, X'ian, China, 4 p.*

[14] S. Nsele, L. Escotte, J.G. Tartarin, S. Piotrowicz, S. Delage. "BroadBand Frequency Dispersion Modeling of the Output Conductance and Transconductance in AlInN/GaN HEMTs", *IEEE Transactions on Electron Devices*, April 2013, Vol. 60, , pp.1372-1378

[15] S. Nsele, L. Escotte, J.G. Tartarin, S. Piotrowicz, S. Delage. "Low-frequency noise in reverse-biased Schottky barriers on InAlN/AlN/GaN heterostructures", *Applied Physics Letters*, Vol.105, N°19, 192105p., Novembre 2014.

[16] J.G. Tartarin, Invited paper "Diagnostic tools for accurate reliability investigations of GaN devices", *International Conference on Noise and Fluctuations (ICNF 2011)*, *IEEE conf.*, pp.456-461.

[17] T. Hisaka, Y. Nogami, H. Sasaki, A. Hasuike, N. Yoshida, K. Hayashi, T. Sonoda, A. Villanueva, J. Del Alamo, "Degradation mechanism of PHEMT under large signal operation", *IEEE GaAs Symposium, 25<sup>th</sup> annual technical Digest 2003*, 4p.